An Inner Centromere Protein that Stimulates the Microtubule Depolymerizing Activity of a KinI Kinesin

Ryoma Ohi,[1,*] Margaret L. Coughlin,[1]
William S. Lane,[2] and Timothy J. Mitchison[1,3]
[1]Department of Cell Biology
Harvard Medical School
Boston, Massachusetts 02115
[2]Harvard Microchemistry Facility
Harvard University
Cambridge, Massachusetts 02138
[3]Institute for Chemistry and Cell Biology
Harvard Medical School
Boston, Massachusetts 02115

Summary

Mitosis requires precise control of microtubule dynamics. The KinI kinesin MCAK, a microtubule depolymerase, is critical for this regulation. In a screen to discover previously uncharacterized microtubule-associated proteins, we identified ICIS, a protein that stimulates MCAK activity in vitro. Consistent with this biochemical property, blocking ICIS function in *Xenopus* extracts with antibodies caused excessive microtubule growth and inhibited spindle formation. Prior to anaphase, ICIS localized in an MCAK-dependent manner to inner centromeres, the chromosomal region located in between sister kinetochores. From *Xenopus* extracts, ICIS coimmunoprecipitated MCAK and the inner centromere proteins INCENP and Aurora B, which are thought to promote chromosome biorientation. By immunoelectron microscopy, we found that ICIS is present on the surface of inner centromeres, placing it in an ideal location to depolymerize microtubules associated laterally with inner centromeres. At inner centromeres, MCAK-ICIS may destabilize these microtubules and provide a mechanism that prevents kinetochore-microtubule attachment errors.

Introduction

Successful duplication of eukaryotic cells requires precise division of their replicated genomes into two equal complements, a process termed mitosis. This is accomplished by attaching paired sister chromatids to the spindle, a bipolar microtubule-based apparatus, which then transports one complete set of chromatids to each pole during anaphase (Scholey et al., 2003). Sister chromatids attach microtubules at kinetochores, specialized proteinacious structures that assemble onto centromeres (Cleveland et al., 2003), and, for accurate chromosome segregation to occur, must do so in such a way that each kinetochore attaches only to microtubules anchored at the pole it faces (Rieder and Salmon, 1998). The steps leading to this configuration, referred to as biorientation, are fueled by microtubule polymerization dynamics (Nicklas, 1997; Rieder and Salmon, 1994). Microtubules are protofilament polymers of $\alpha\beta$-tubulin

*Correspondence: ryoma_ohi@hms.harvard.edu

heterodimers that exhibit dynamic instability, a nonequilibrium behavior where polymerizing and depolymerizing microtubules coexist and transit stochastically between these states (Desai and Mitchison, 1997). This enables microtubules to rapidly and efficiently explore three-dimensional space (Holy and Leibler, 1994), a key property exploited during spindle assembly (Hyman and Karsenti, 1996; Karsenti and Vernos, 2001) and "capture" of microtubules by kinetochores (Kirschner and Mitchison, 1986). Microtubules assembled from pure tubulin in vitro exhibit dynamic instability, but their dynamics parameters differ significantly in vivo, indicating regulation by cellular factors (Cassimeris, 1999).

MCAK/XKCM1 (hereafter referred to as MCAK because they are orthologs) is a KinI kinesin (Walczak et al., 1996; Wordeman and Mitchison, 1995), that is, it contains an internal motor domain. Unlike transport kinesins, KinIs use ATP hydrolysis to disassemble microtubules from their ends (Desai et al., 1999b; Hunter et al., 2003). Studies in *Xenopus* extracts (Walczak et al., 1996) and cells (Kline-Smith and Walczak, 2002) have shown that MCAK employs this activity to induce microtubule catastrophes, the transition from growth to shrinkage. MCAK is crucial for "global" microtubule dynamics regulation throughout mitotic cytoplasm, and, in combination with the polymerization promoting factor XMAP215 (Gard and Kirschner, 1987), can reconstitute near physiological microtubule dynamics in vitro (Kinoshita et al., 2001).

MCAK (*m*itotic *c*entromere-*a*ssociated *k*inesin) is a centromeric KinI (Walczak et al., 1996; Wordeman and Mitchison, 1995), so we expect that MCAK has local functions at centromeres in addition to its more global role in microtubule dynamics regulation. Antisense (Maney et al., 1998) and dominant-negative experiments (Maney et al., 1998; Walczak et al., 2002) suggested possible functions for centromere-bound MCAK in poleward movement of chromatids during anaphase and in chromosome alignment, respectively. The details of these functions, and whether they depend on MCAK at centromeres or at kinetochores, are not known. In addition, the spatial, physical, and functional relationships between MCAK and other centromere proteins remain unexplored. In this paper, we report the identification of ICIS (*I*nner *C*entromere Kin*I S*timulator), a protein that targets inner centromeres in an MCAK-dependent manner. In *Xenopus* extracts, ICIS associates with MCAK and the inner centromere proteins INCENP and Aurora B, proteins thought to be important for chromosome biorientation (Tanaka, 2002). ICIS stimulates MCAK activity in vitro, suggesting that ICIS may regulate MCAK at inner centromeres. We hypothesize a third, inner centromere-specific function of MCAK, in which it works with ICIS to promote biorientation by preventing kinetochore-microtubule attachment errors.

Results

Identification of ICIS as a MAP from *Xenopus* Extracts
To identify mitotic microtubule regulating proteins, we purified proteins that bind microtubules rapidly and with
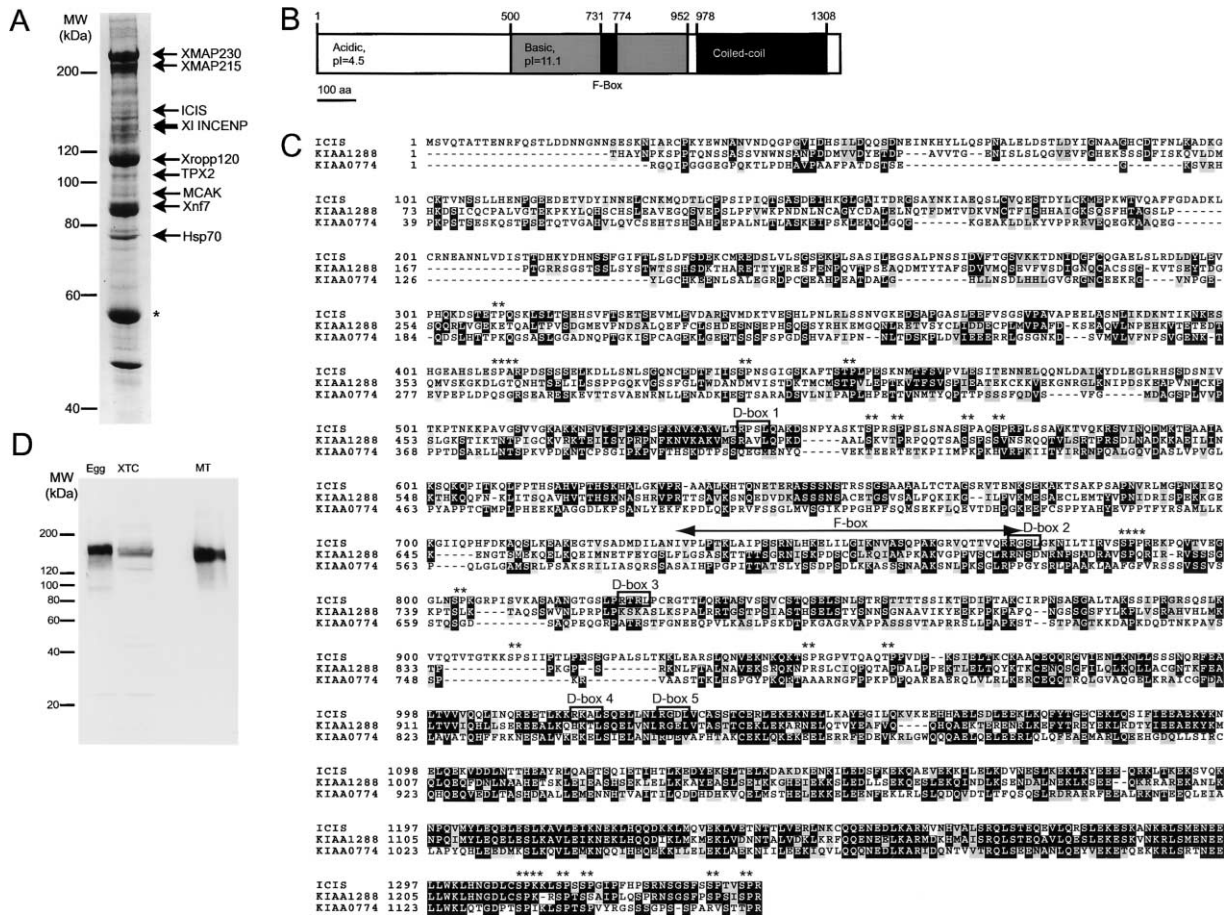
Figure 1. ICIS Is a *Xenopus* MAP

(A) Coomassie blue staining of MAPs prepared from clarified *Xenopus* CSF extract. Proteins identified by immunoblotting or mass spectrometry are indicated. The asterisk denotes tubulin.

(B) Domain organization of ICIS.

(C) Sequence alignment of *Xenopus laevis* ICIS with human KIAA1288 and KIAA0774. Dark shading indicates identical residues and light shading indicates conserved residues. The F box in ICIS (Regan-Reimann et al., 1999) is marked with a double arrow. Putative destruction boxes and Cdc2 phosphorylation sites are denoted by boxes and asterisks, respectively.

(D) Specificity of α-ICIS antibody. CSF extract (Egg), lysate prepared from asynchronous XTC cells (XTC), and MAPs prepared from high-speed supernatant of CSF extract (MT) were immunoblotted with affinity-purified α-ICIS.

high affinity from *Xenopus* egg extracts that are naturally arrested at meiosis II metaphase (CSF extract). Taxol-stabilized GMPCPP-microtubules were briefly incubated in high-speed supernatants of CSF extract at 0°C, and then isolated by two rounds of centrifugation through sucrose cushions. Bound proteins were eluted with high salt and analyzed by SDS-PAGE.

Approximately 30 major polypeptides were reproducibly recovered (Figure 1A). Nine were identified using both immunoblotting and protein sequencing by ion trap mass spectrometry. Of these, six are known microtubule-associated proteins (MAPs; Figure 1A and Supplemental Data at http://www.developmentalcell.com/cgi/content/full/5/2/309/DC1), confirming specificity of the assay. Tandem mass spectrometry of tryptic peptides derived from one ~150 kDa protein revealed that it is an uncharacterized MAP, though part of the protein had previously been isolated by two-hybrid interaction with Skp1 (Regan-Reimann et al., 1999). Skp1 interacts with many proteins through a motif termed the F box (Bai et al., 1996),

and, accordingly, this clone was named Fbx27. We have redesignated Fbx27 ICIS to reflect its MCAK-stimulating activity in vitro, and present its preliminary characterization here.

Primary Structure of ICIS
A full-length cDNA encoding ICIS predicted a 147 kDa polypeptide of 1338 amino acids with homology to two human proteins of unknown function, KIAA1288 and KIAA0774 (Figure 1C). ICIS is organized into three regions of roughly equivalent size (Figure 1B). The N-terminal (residues 1–500) and central (residues 501–952) regions have acidic (pI = 4.5) and basic (pI = 11.1) isoelectric points, respectively, while the C terminus (residues 978–1308) predicts a coiled coil. The previously identified F box in ICIS (Regan-Reimann et al., 1999) is located between residues 731–774 (Figures 1B and 1C).

To study the mitotic function of ICIS, antibodies were generated against ICIS amino acid residues 727–1065 and affinity purified. Immunoblotting of *Xenopus* CSF

extract, lysate derived from asynchronous *Xenopus* XTC cells, and our XMAP preparation with α-ICIS antibodies all detected a single $\sim$150 kDa protein (Figure 1D). ICIS is fairly abundant in CSF extract. By quantitative immunoblotting, we estimate that the concentration of ICIS is $\sim$80 μg/ml, or $\sim$500 nM.

Localization of ICIS during Mitosis
We examined the localization of ICIS during mitosis by immunofluorescence. In XTC cells, ICIS is either absent or weakly nuclear in most interphase cells (data not shown). During prophase, ICIS is detected exclusively on centrosomes, where it is observed throughout the remaining stages of mitosis (Figure 2A). During prometaphase, uniform puncta of ICIS are also detected on chromosomes, which suggests centromere localization. ICIS remains associated with metaphase chromosomes but in contrast to its appearance during prometaphase, is observed as irregularly shaped patches of varying lengths and brightness. Chromosomal staining disappears in anaphase cells. Finally, during telophase, ICIS is located at the midbody.

ICIS localization is similar on metaphase spindles assembled in vitro using *Xenopus* extracts (Figure 2B). Bright, punctate staining was observed on chromosomes and weak staining was seen on spindle poles. By comparing ICIS localization to that of XCENP-E, a kinesin located at kinetochores (Wood et al., 1997), it was evident that ICIS was positioned in between paired sister kinetochores, that is, at inner centromeres (Cleveland et al., 2003). Consistently, ICIS staining was indistinguishable from that of Aurora B (Figure 2D), an established inner centromere protein (Adams et al., 2001; Cleveland et al., 2003; Shannon and Salmon, 2002).

Perturbing ICIS Function Disrupts Assembly and Structural Integrity of the Mitotic Spindle
We explored ICIS function in spindle assembly using *Xenopus* extracts. To date, we have been unable to completely remove ICIS by immunodepletion. Furthermore, partial immunodepletion codepletes associated proteins known to be important for spindle assembly (see below), complicating interpretation of phenotypic effects. Therefore, we focused on the effects of adding α-ICIS antibodies to extracts to block its function(s). Adding affinity-purified α-ICIS (0.75 mg/ml) to CSF extracts blocked normal spindle assembly. Instead, huge microtubule asters and disorganized microtubule aggregates assembled around condensed chromosomes (Figure 3A).

To quantify the effect of α-ICIS addition, we examined spindle assembly in cycled extracts because this process is reproducibly more robust in cycled extracts than in CSF extracts. In control extracts, the majority of assembled structures were bipolar spindles with chromosomes aligned at the metaphase plate (Figures 3B and 3C). In contrast, α-ICIS-containing extracts were unable to support spindle assembly. Instead, we observed dense microtubule aggregates of indeterminate polarity that enveloped condensed, randomly oriented chromosomes (Figures 3B and 3C). Long microtubules emanated from the periphery of a subset of these aggregates, and in extreme cases produced large microtubule asters similar to those observed in CSF extracts (Figure 3B).

To determine whether ICIS function is required once spindle assembly and chromosome alignment have been completed, we added α-ICIS (0.5 mg/ml) to cycled extracts containing bipolar metaphase spindles. Within 5 min, excessive microtubule polymerization was evident throughout the spindle (data not shown). Abnormal polymerization was accompanied by displacement of chromosomes from the metaphase plate and structural deformation of the spindle (Figures 3D and 3E). Disruption of chromosome alignment was not due to premature loss of sister chromatid cohesion or induction of anaphase because sister kinetochores remained paired in perturbed structures (data not shown). These results implicate ICIS in microtubule dynamics regulation during mitosis, but do not distinguish whether its role is direct or indirect.

ICIS Associates with Inner Centromere Proteins and Skp1
To further explore ICIS function, we identified polypeptides that coimmunoprecipitated with ICIS from CSF extracts by mass spectrometry (Figure 4A). We identified one protein that might be relevant to the microtubule dynamics effect of ICIS perturbation (XKCM1, the *Xenopus* ortholog of MCAK), two consistent with a function for ICIS at inner centromeres (Aurora B and INCENP), and one consistent with the F box being functional (Skp1). The interaction of MCAK with ICIS was confirmed by immunoblot analyses of reciprocal coimmunoprecipitation experiments (Figure 4B). We also confirmed the presence of INCENP, Aurora B, and Skp1 in α-ICIS immunoprecipitates by immunoblot analysis (Figure 4C).

To determine whether the association between ICIS and MCAK is relevant in intact spindles, we stained spindles assembled in vitro with antibodies specific for both MCAK and ICIS. Identical staining of inner centromeres was observed (Figure 4D), consistent with the two proteins physically interacting at this location.

ICIS Inner Centromere Localization Depends on MCAK
We compared the kinetics of ICIS and MCAK accumulation at inner centromeres in XTC cells by immunofluorescence (Figure 5A). MCAK was observed at kinetochores or inner centromeres in a small fraction of interphase cells that were presumably in late G_2. In these cells, ICIS was only detected on centrosomes. During prophase, MCAK localization persisted at kinetochores or inner centromeres, and also overlapped with ICIS staining at centrosomes. Extensive colocalization of MCAK and ICIS at both inner centromeres and centrosomes was evident in prometaphase and metaphase cells. Thus, MCAK accumulates at inner centromeres before ICIS in vivo.

Because MCAK localizes to inner centromeres first, we tested whether MCAK is required for inner centromere targeting of ICIS. Egg extract was immunodepleted using α-MCAK or control antibodies (Figure 5B), and then used to assemble mitotic chromosomes in the presence of nocodazole to prevent microtubule polymerization. By immunofluorescence, MCAK and ICIS colocalized on chromosomes assembled in mock-
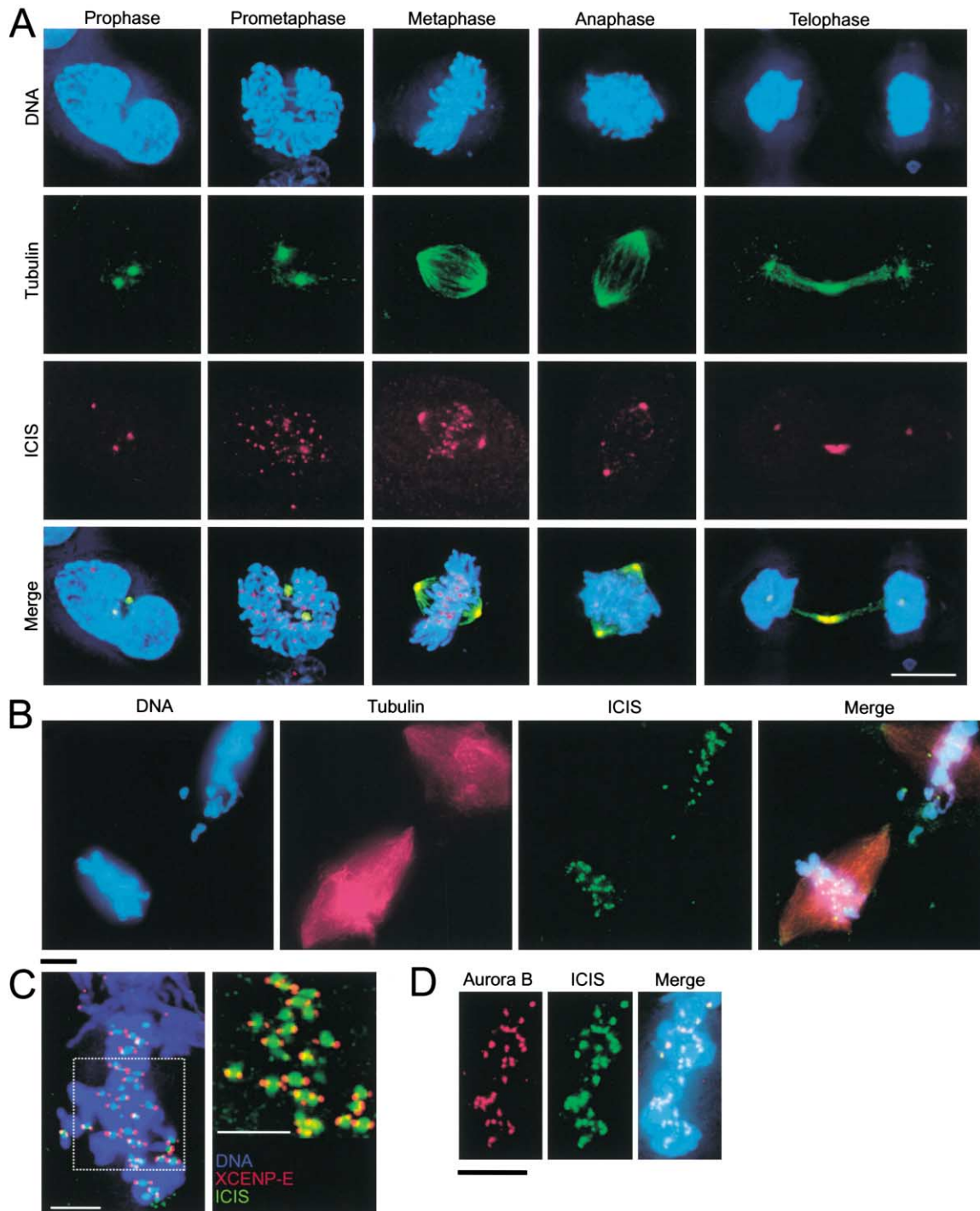
Figure 2. ICIS Localization during Mitosis

(A) Localization of ICIS in XTC cells during mitosis. Cells were fixed and processed for immunofluorescence with α-ICIS and α-tubulin antibodies. DNA was visualized with Hoechst 33342. The scale bar represents 10 μm.

(B) ICIS localization on spindles assembled in vitro. Rhodamine-tubulin-labeled metaphase spindles assembled using *Xenopus* extract were fixed and stained with α-ICIS and Hoechst 33342. The scale bar represents 10 μm.

(C) ICIS localizes between sister kinetochores. Metaphase spindles assembled in vitro were fixed and stained with α-ICIS and α-XCENP-E antibodies. The boxed region is enlarged and shown without DNA staining (right) to depict ICIS and XCENP-E localization more clearly. The scale bars represent 5 μm.

(D) ICIS colocalizes with Aurora B. Metaphase spindles assembled in vitro were fixed and double stained with α-ICIS and α-Aurora B antibodies. The scale bar represents 10 μm.
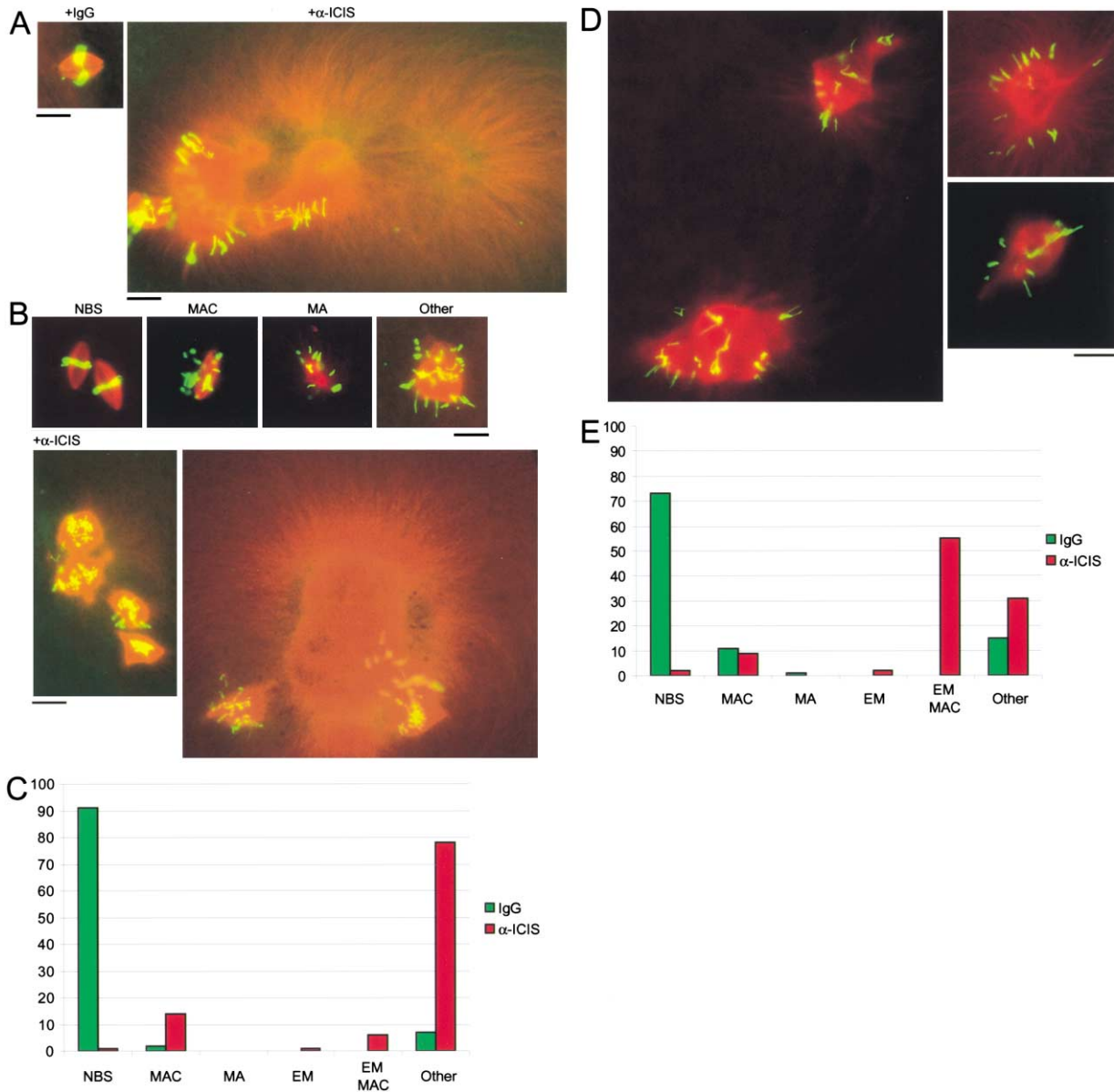
Figure 3. ICIS Perturbation Disrupts Assembly and Structural Integrity of the Spindle

(A) Effect of α-ICIS on spindle assembly in CSF extracts. Representative structures assembled in the presence of 0.75 mg/ml random IgG or α-ICIS are shown. Microtubules (red) were visualized with rhodamine-tubulin and DNA (green) with Hoechst 33342. The scale bar represents 25 μm.

(B) α-ICIS prevents spindle assembly in cycled extracts. CSF extract containing sperm nuclei and either 0.75 mg/ml IgG or α-ICIS were cycled through interphase and rearrested at metaphase. Representative structures are shown. The scale bar represents 25 μm. Spindle classification: NBS, normal bipolar spindle; MAC, bipolar spindle with misaligned chromosomes; MA, monoastral structures; Other, chromosomes associated with microtubules of indeterminate organization.

(C) Quantitation of structures formed during cycled spindle assembly in the presence of IgG or α-ICIS. Similar results were obtained in three independent experiments. Classification as in (B) with the addition of EM, denoting spindles surrounded by excessive microtubules.

(D) Addition of α-ICIS to preassembled spindles disrupts metaphase chromosome alignment and spindle architecture. IgG or α-ICIS was added to bipolar spindles to 0.5 mg/ml and incubated at 20°C for 30 min. The scale bar represents 10 μm.

(E) Quantitation of spindle morphologies observed 30 min following addition of either IgG or α-ICIS. Spindle classifications are as in (B) and (C). Similar results were obtained in five independent experiments.

depleted extract (Figure 5C). Thus, microtubules are not required for ICIS to localize to inner centromeres. MCAK immunofluorescence was abolished on chromosomes assembled in MCAK-depleted extract. MCAK immunodepletion also eliminated ICIS staining despite the fact that ICIS abundance was unchanged relative to control extracts (Figure 5B), indicating that ICIS requires MCAK to target inner centromeres. We were unable to perform the reciprocal immunodepletion, as discussed above.

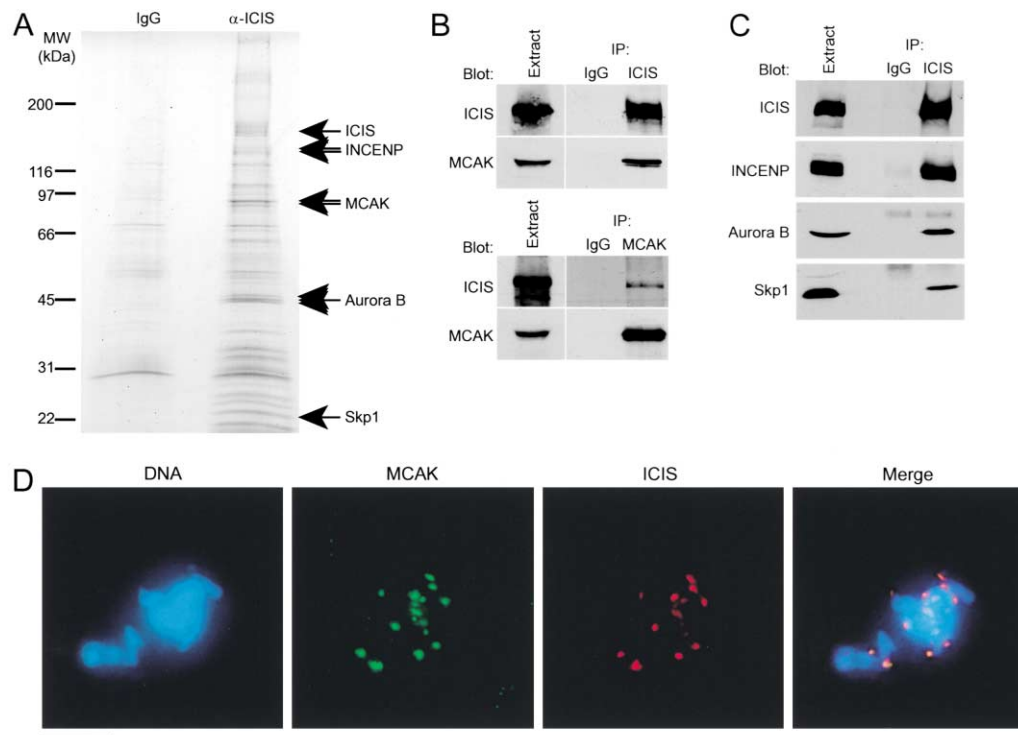To verify the ICIS inner centromere-targeting function

Figure 4. ICIS Associates with Inner Centromere Proteins in *Xenopus* Extract

(A) α-ICIS immunoprecipitates contain INCENP, MCAK, Aurora B, and Skp1. IgG and α-ICIS immunoprecipitates from CSF extract were analyzed by Coomassie blue staining. Indicated protein bands were identified by ion trap mass spectrometry.

(B) Reciprocal coimmunoprecipitation of ICIS and MCAK. IgG, α-ICIS, and α-MCAK immunoprecipitates from CSF extract were immunoblotted with α-ICIS or α-MCAK.

(C) Validation of INCENP, Aurora B, and Skp1 coimmunoprecipitation by immunoblotting. IgG and α-ICIS immunoprecipitates were probed with α-INCENP, α-Aurora B, and α-Skp1 antibodies.

(D) ICIS colocalizes with MCAK. Metaphase spindles assembled in vitro were fixed and processed for immunofluorescence using α-ICIS and α-MCAK antibodies. The scale bar represents 10 μm.

of MCAK, we used a dominant-negative approach. Spindles were assembled in the presence of the N terminus of MCAK, MCAK^NT, which displaces MCAK from inner centromeres without affecting spindle assembly (Walczak et al., 2002). As expected, MCAK inner centromere staining was abolished by MCAK^NT, but was unaffected in control spindles formed in the presence of GST. Similarly, ICIS was displaced from inner centromeres by MCAK^NT, but not by GST (Figure 5D). Collectively, these data show that ICIS inner centromere targeting requires MCAK but not microtubules.

MCAK Activity Is Stimulated by ICIS
To test whether ICIS has an effect on MCAK function, full-length ICIS and *Xenopus* MCAK were separately expressed and purified (Figure 6A), and various combinations of the two proteins were analyzed for their ability to depolymerize GMPCPP-stabilized microtubules. We assayed microtubule disassembly qualitatively using fluorescent GMPCPP-microtubules at 1.5 μM tubulin, 15 nM MCAK (dimer concentration), and 50 nM ICIS. ICIS alone had no noticeable effect on GMPCPP-microtubule stability. MCAK alone caused ATP- and time-dependent microtubule depolymerization. Interestingly, ICIS stimulated the rate at which MCAK disassembled polymer (Figure 6B). This reproducible effect was evident at early

time points and was clearest ~10 min following initiation of the reaction when complete microtubule depolymerization had occurred. ICIS did not obviate the ATP requirement for MCAK activity, and AMPPNP inhibited the three-component reaction (data not shown). In titration experiments scored at a single time point, we found that the stimulatory effect of ICIS could be detected at protein concentrations as low as 3 nM, one-fifth the concentration of MCAK (Figure 6C). From these data, we conclude that ICIS stimulates MCAK activity at concentrations substoichiometric to that of MCAK and protofilament ends (~12 nM; calculated assuming 2 μm average microtubule length, 1750 tubulin dimers/μm, and 28 protofilament ends/microtubule; Hunter et al., 2003).

We tested whether ICIS binds microtubules, as this property might be relevant to its MCAK-stimulatory activity. Pure ICIS was incubated with unpolymerized tubulin or microtubules, and the protein mixtures were centrifuged over sucrose cushions. Unpolymerized tubulin remained in the supernatant whereas ~50% of ICIS was detected in the pellet of the same sample. We suspect that this is due to oligomerization of ICIS, as we have observed regular oligomers in preliminary EM experiments (our unpublished data). However, all detectable ICIS cosedimented with microtubules (Figure 6D), suggesting that ICIS binds microtubules directly.
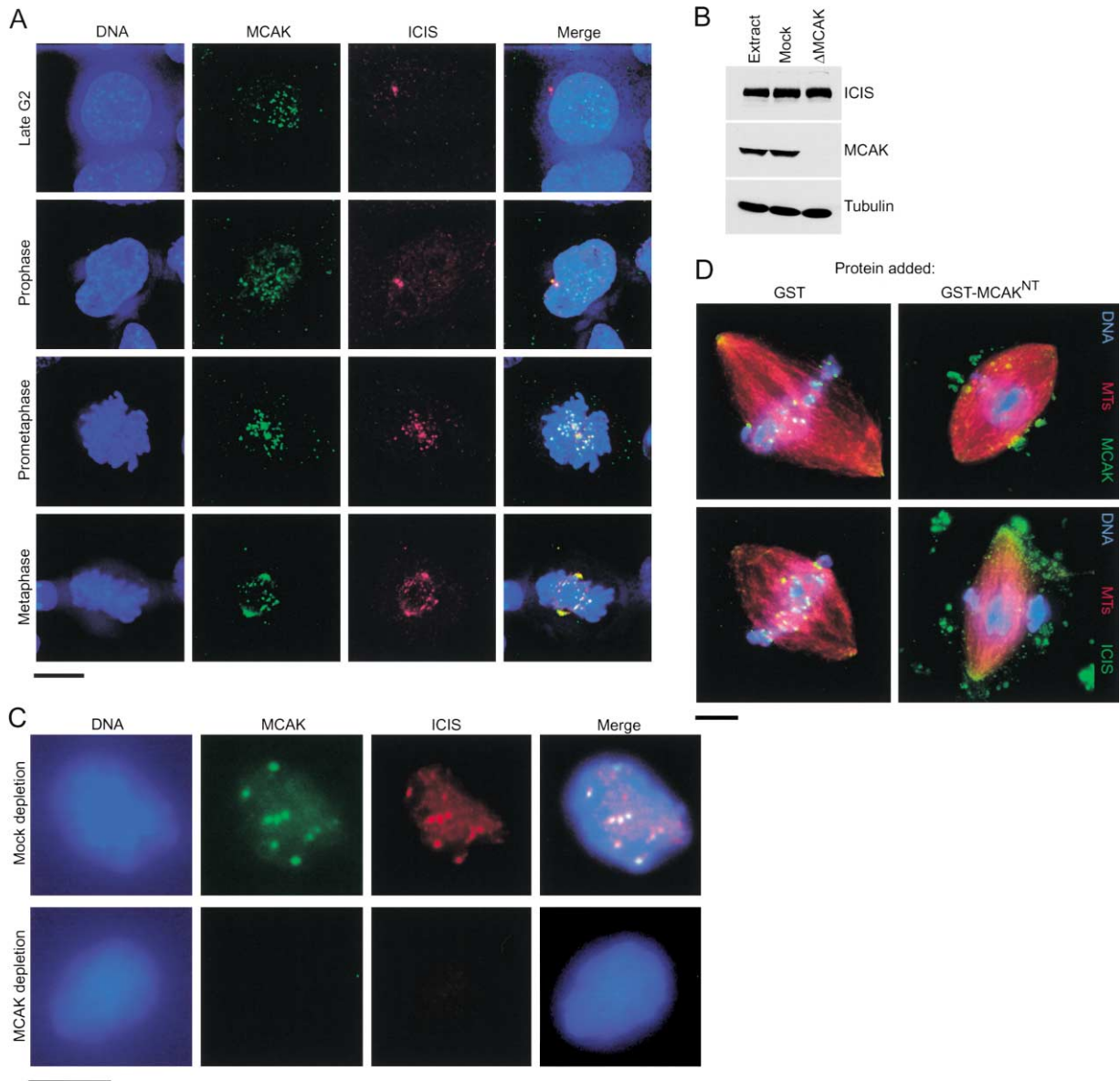
Figure 5. ICIS Inner Centromere Localization Requires MCAK

(A) Comparison of MCAK and ICIS localization during preanaphase mitosis. XTC cells were fixed and double stained with α-MCAK and α-ICIS. DNA was counterstained with Hoechst 33342. The scale bar represents 10 μm.

(B) Immunodepletion of MCAK. An immunoblot of 0.5 μl of unmanipulated extract (Extract), extract depleted using IgG (Mock), or α-MCAK (ΔMCAK) was probed with α-ICIS, α-MCAK, and α-tubulin.

(C) Inner centromere targeting of ICIS requires MCAK. Chromosomes assembled in *Xenopus* extract depleted using either IgG or α-MCAK in the presence of nocodazole were processed for immunofluorescence using α-MCAK and α-ICIS. DNA was stained with Hoechst 33342. The scale bar represents 10 μm.

(D) GST-MCAK^NT displaces ICIS from inner centromeres. Spindles assembled in the presence of GST or GST-MCAK^NT were fixed and stained with α-MCAK-CTP or α-ICIS. The scale bar represents 10 μm.

ICIS Is Located on the Surface of Inner Centromeres

To help determine the relevant population(s) of microtubules that are destabilized at inner centromeres by MCAK-ICIS, we localized ICIS in metaphase spindles assembled in vitro by immunoelectron microscopy. As in other vertebrates, inner centromeres were located between kinetochores (Cleveland et al., 2003; Cooke et al., 1987), evident by their trilaminar appearance and attachment to kinetochore fiber microtubules (Figure 7A). Kinetochore fibers were associated with microtubules that did not terminate at kinetochores, and instead interacted laterally with inner centromeres (Figure 7A, arrowheads). Laterally associated microtubules were observed in 100% of the ~50 kinetochore pairs examined by serial section electron microscopy from approximately three different experiments. Similar laterally associated microtubules have been reported in *Haemanthus*
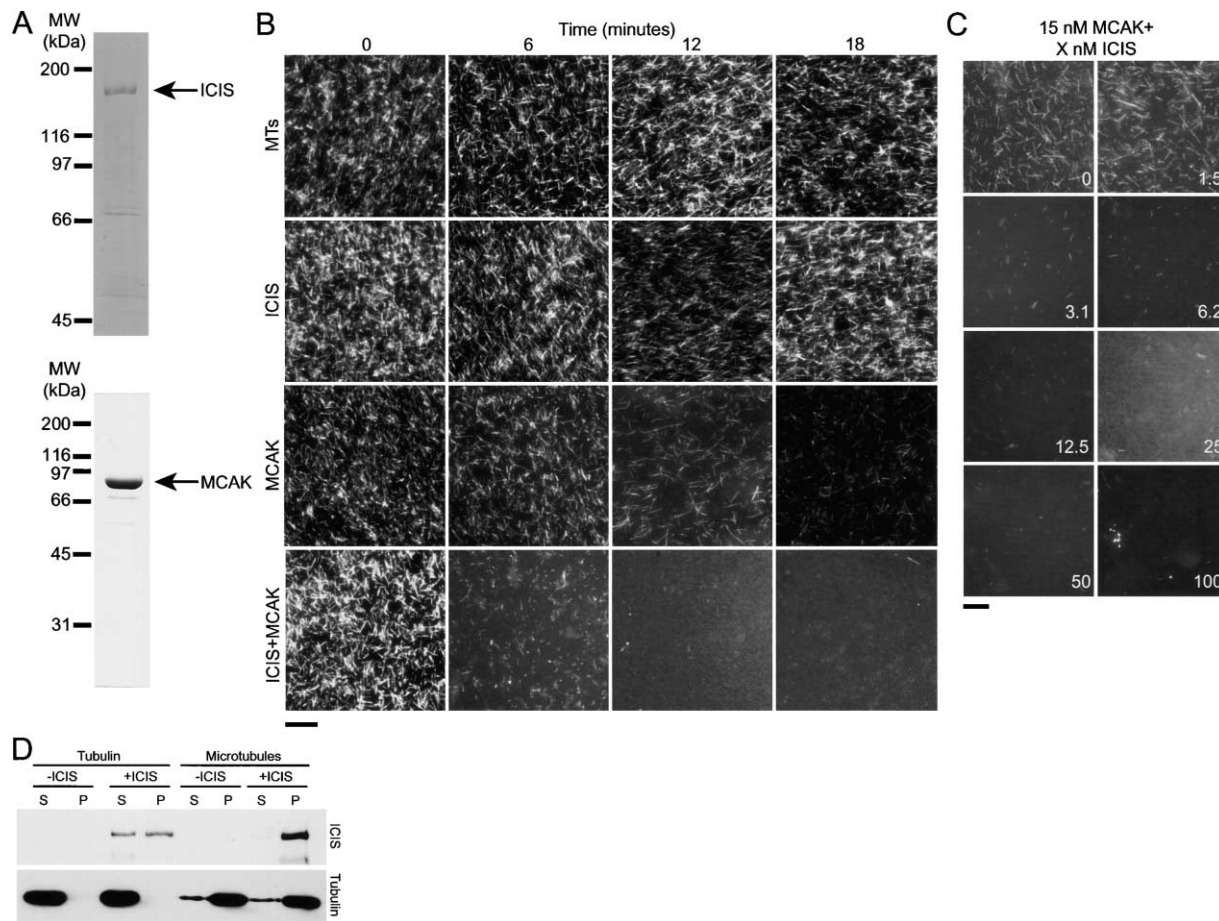
Figure 6. ICIS Stimulates the Microtubule Depolymerizing Activity of MCAK

(A) Purification of recombinant *Xenopus* ICIS and MCAK. Coomassie blue staining of 2.5 μg of ICIS and MCAK separately expressed and purified from *Sf*-9 cells is shown.

(B) ICIS stimulates MCAK activity. Rhodamine-labeled GMPCPP-microtubules (1.5 μM tubulin) were mixed with 50 nM ICIS, 15 nM MCAK, or both proteins and analyzed by fluorescence microscopy after incubation at 22°C for the indicated amounts of time. The scale bar represents 10 μm.

(C) ICIS stimulates MCAK substoichiometrically. MCAK (15 nM) was mixed with varying concentrations of ICIS (nM concentrations are indicated in each panel) and 1.5 μM GMPCPP-microtubules. Panels show representative fields following an 18 min incubation at 22°C. The scale bar represents 10 μm.

(D) ICIS cosediments with microtubules. Pellet (P) and supernatant (S) fractions from ICIS-containing tubulin/microtubule copelleting assays were analyzed by immunoblotting with α-tubulin and α-ICIS.

and PtK1 kinetochore fibers (Jensen, 1982; McDonald et al., 1992).

To image ICIS, we labeled spindles with α-ICIS during their assembly at a concentration (10 μg/ml) that does not affect spindle assembly. After fixation, bound antibodies were detected using nanogold-conjugated secondary antibodies followed by silver enhancement. Figure 7B is a low-magnification view of the sister chromatid pair subjected to serial sectioning presented in Figure 7C. Strong antibody labeling was detected at inner centromeres. By analyzing serial 85 nm sections, it was evident that label was present both on the surface and embedded throughout the chromatin in the region of the centromere (Figure 7C).

There was a strong correlation between silver deposits and the presence of microtubules, which was especially apparent at the surface of inner centromeres (Figure 7C). In addition, ICIS labeling was observed on microtubules that were in close proximity to chromosomes (Figure 7C, arrowheads). We did not observe

inner centromere and microtubule staining using random IgG as the primary antibody, showing that the immunolabeling was specific (data not shown).

Discussion

ICIS Is an Inner Centromere Protein that Stimulates the Microtubule Depolymerizing Activity of MCAK

We identified ICIS as a MAP from metaphase *Xenopus* extracts. ICIS is conserved in vertebrates, being orthologous to KIAA1288 and homologous to KIAA0774, two human proteins of unknown function. Related proteins are not detectable in invertebrates, but it is likely that they exist because ICIS associates with the widely conserved proteins INCENP, Aurora B, and MCAK. Notably, the F box in ICIS is not well conserved in KIAA1288 or KIAA0774 (Figure 1C). It is unclear whether this reflects the sequence degeneracy typically observed among F boxes (Bai et al., 1996) or whether this motif is moved
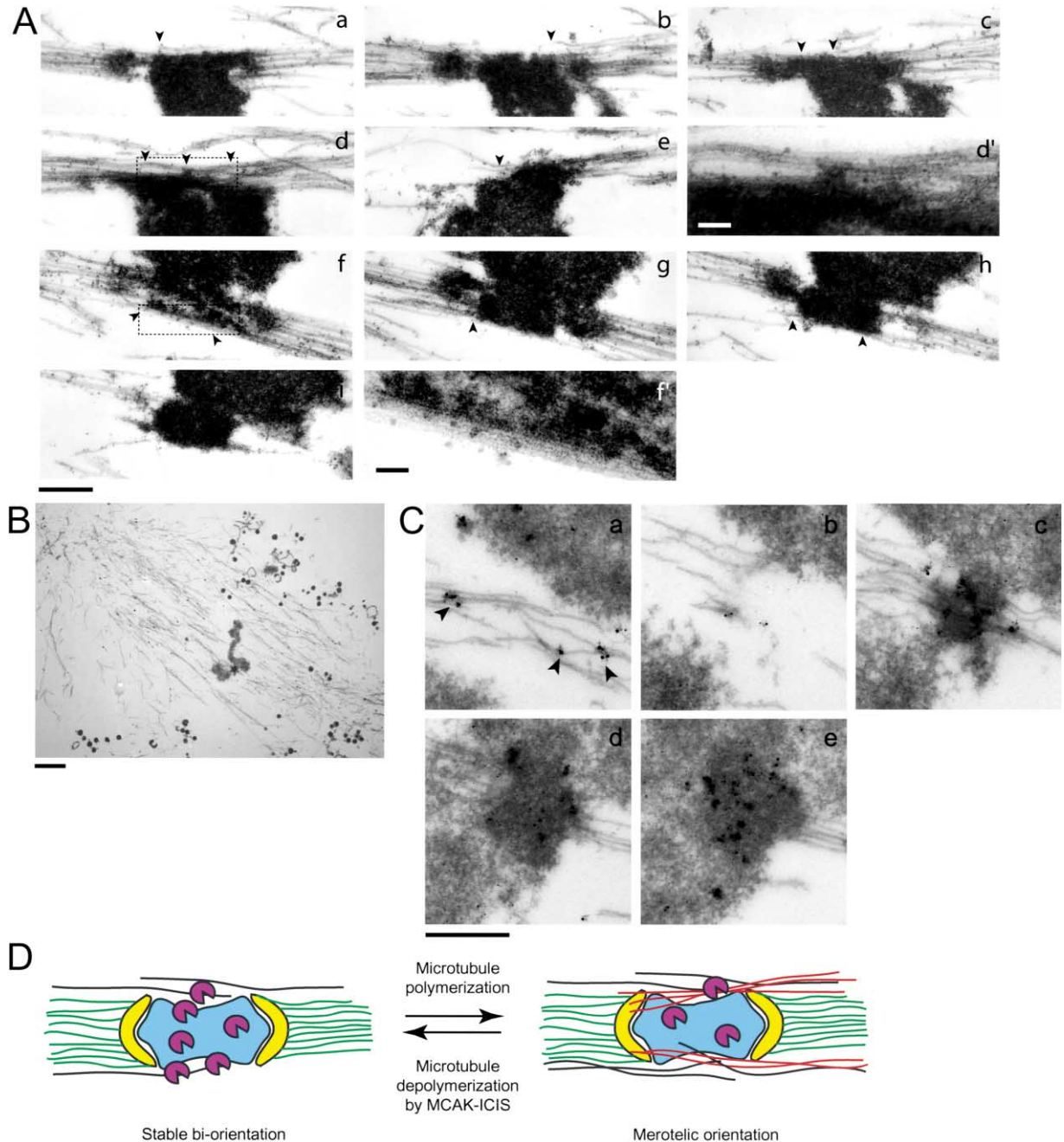
Figure 7. ICIS Localization at Inner Centromeres by Immunoelectron Microscopy

(A) Microtubules flank inner centromeres in *Xenopus* extract spindles. Longitudinal 85 nm serial sections through two pairs of sister chromatids (a–e and f–i) are presented. Kinetochores are recognizable by their morphology and attachment to kinetochore fibers. Note microtubules that associate with pericentric chromatin (arrowheads) without apparent termination at kinetochores. Boxed regions in "d" and "f" are enlarged in "d'" and "f'" to better illustrate laterally associated microtubules. The scale bars represent 500 nm (a–i) and 100 nm (d' and f').
(B) Low-magnification view of the spindle subjected to serial section analysis in (C). The scale bar represents 2 μm.
(C) ICIS localization by immunoelectron microscopy. Spindles labeled with α-ICIS were fixed and processed for immunoelectron microscopy. Panels represent serial 85 nm longitudinal sections through one sister chromatid pair. Arrowheads denote immunolabeling on microtubules that flank the inner centromere. The scale bar represents 500 nm.
(D) Model. Positioned at the surface of inner centromeres (blue), MCAK-ICIS (purple) could prevent kinetochore (yellow)-microtubule attachment errors (e.g., merotelic orientation) by depolymerizing microtubules that extend beyond the kinetochore facing the pole from which it originates (black). Microtubules attached to the incorrect kinetochore are shown in red.

or absent in the human proteins. Skp1 coimmunoprecipitates with ICIS and interacts with ICIS in the two-hybrid system (Regan-Reimann et al., 1999). Thus, the ICIS F box is likely functional.

During prometaphase and metaphase, ICIS localizes to inner centromeres in an MCAK-dependent manner. This region of paired sister chromatids maintains their cohesion prior to anaphase (Nasmyth et al., 2000),

and promotes chromosome biorientation through the INCENP-Aurora B-Survivin complex (Shannon and Salmon, 2002; Tanaka, 2002). How this complex contributes to biorientation is not known, but recent studies have proposed that Aurora B-dependent regulation of microtubule dynamics may be involved (Buvelot et al., 2003; Kallio et al., 2002). ICIS immunoprecipitates from egg extracts contain INCENP and Aurora B, suggesting that ICIS may cooperate with INCENP-Aurora B to biorient sister chromatids.

In vitro, ICIS stimulates the microtubule-destabilizing activity of MCAK. This is consistent with the microtubule assembly-promoting effect that α-ICIS antibodies have when added to egg extracts, and the observations that MCAK and ICIS colocalize at inner centromeres and physically associate in extract. Based on the MCAK-stimulating activity of ICIS and the association of IN-CENP, Aurora B, and MCAK with ICIS, we speculate that Aurora B may affect microtubule dynamics, at least in part, through phosphorylation-dependent regulation of MCAK-ICIS.

Biochemistry of MCAK Regulation by ICIS

An important issue concerns the mechanism by which ICIS stimulates MCAK. ICIS could improve the processivity of MCAK, which removes ~20 dimers from a protofilament before dissociating (Hunter et al., 2003) by anchoring it to microtubules during catalysis. That ICIS binds microtubules independently of MCAK is consistent with such a mechanism. A second consideration is that MCAK has affinity for free dimers, and the MCAK-dimer complex is a normal byproduct of microtubule depolymerization (Desai et al., 1999b). ICIS could facilitate MCAK-dimer dissociation, thereby preventing product inhibition.

Because MCAK is highly active as a pure protein (Desai et al., 1999b; Hunter et al., 2003), why would it require a stimulatory factor? In vitro, ICIS activity is most apparent at high polymeric tubulin concentrations (>1 μM), which is probably relevant within the spindle where concentrations of tubulin and microtubules are likely higher than those typically used to assay KinIs in vitro. Further, spindle microtubules may be more difficult to depolymerize than the pure microtubules used to analyze KinI activity because of their association with MAPs. Finally, two levels of MCAK potency, one driven by the inherent activity of MCAK and the other produced by ICIS stimulation, may allow for more exquisite regulation of microtubule disassembly by MCAK.

Lateral Microtubule-Inner Centromere Interactions and MCAK-ICIS

The importance of MCAK regulation by ICIS at inner centromeres has been difficult to assess because MCAK also regulates global microtubule dynamics (Walczak et al., 1996). Perturbing ICIS in metaphase spindles caused abnormal microtubule assembly, an effect consistent with global MCAK inhibition rather than specific inhibition at inner centromeres. However, we suspect that this effect is indirect, mediated by recruitment of MCAK to IgG-ICIS aggregates. Blocking MCAK inner centromere localization perturbs chromosome alignment without significantly affecting global microtubule dynamics

(Walczak et al., 2002). MCAK[NT] also interferes with MCAK-ICIS association (R.O. and T.J.M., unpublished data), suggesting that ICIS may not be important for global microtubule dynamics regulation and may be more relevant for MCAK regulation at inner centromeres. Further clarification of these issues requires efficient methods to block MCAK-ICIS association without interfering with other potential functions of ICIS at inner centromeres.

At inner centromeres, which microtubules do MCAK-ICIS depolymerize and why? Our immunoelectron microscopy data place ICIS at the surface of the inner centromere, an ideal location for MCAK-ICIS to destabilize microtubules associated laterally with inner centromeres. Kinetochore fiber microtubules that do not terminate at kinetochores but rather contact the centromere laterally, are abundant in *Xenopus* extract meiosis II spindles (Figure 7A), and have been documented in *Haemanthus* endosperm and PtK1 cells (Jensen, 1982; McDonald et al., 1992). These microtubules have been ignored in most discussions of the forces acting on kinetochores, and their function is unknown. Without proper dynamics regulation, microtubules associated laterally with inner centromeres could attach an inappropriate kinetochore, leading to chromosome missegregation. We propose that one function of MCAK-ICIS may be to destabilize microtubules associated laterally with inner centromeres (Figure 7D), and in doing so may contribute to prevention of malattachments. Such a mechanism may be especially critical to prevent merotelic orientation, where a kinetochore is attached to microtubules derived from both poles, because this type of error is not detected by the spindle checkpoint (Cimini et al., 2001).

Experimental Procedures

Preparation of *Xenopus* Egg Extracts

CSF extracts were prepared as described (Murray, 1991). For isolation of MAPs, extracts were diluted 3× with CSF-XB (Murray, 1991) containing LPC (10 μg/ml each of leupeptin, pepstatin, and chymostatin), 10 μg/ml cytochalasin D, 1× energy mix (Murray, 1991), and centrifuged at 202,000 × g for 20 min. The cytoplasmic fraction was centrifuged again at the same speed for 10 min, frozen in liquid nitrogen, and stored at −80°C.

Isolation of XMAPs

Clarified CSF extracts were thawed, incubated with 50 μM nocodazole at 0°C for 30 min, and then centrifuged for 1 hr at 238,000 × g. The supernatant (1.0 ml) was adjusted to 5 μM taxol and mixed with 3 μM taxol-stabilized GMPCPP-microtubules. After 5 min at 0°C, microtubules were sedimented through a 1.2 ml 40% sucrose cushion in BRB80 (80 mM K-PIPES [pH 6.8], 1 mM MgCl$_2$, 1 mM EGTA) plus 50 μM nocodazole, 10 μM taxol, 1 mM DTT, LPC, 10 μg/ml cytochalasin D at 238,000 × g for 1 hr. The pellet was resuspended in 150 μl of BRB80 plus 50 μM taxol, 1 mM DTT, LPC and centrifuged through two 150 μl 40% sucrose/BRB80 cushions plus 50 μM taxol, 1 mM DTT, LPC, 10 μg/ml cytochalasin D at 191,000 × g for 30 min. Microtubule-bound proteins were eluted by resuspending the pellet in 20 mM Na-HEPES (pH 6.8), 500 mM NaCl, 5 mM MgATP, 1 mM EGTA, 20 μM taxol, 1 mM DTT, LPC and incubating at 22°C for 30 min. Microtubules were pelleted and proteins in the supernatant were analyzed by SDS-PAGE after precipitation with trichloroacetic acid.

Nano-LC Ion Trap Tandem Mass Spectrometry and Sequencing

Polypeptides were subjected to in-gel reduction, carboxyamidomethylation, and tryptic digestion (Promega). Multiple peptide sequences were determined in a single run by microcapillary reverse-phase chromatography directly coupled to a ThermoFinnigan LCQ

DECA quadrupole ion trap mass spectrometer equipped with a cus-tom nanoelectrospray source. The column, packed in-house with 5 cm of C18 support in a New Objective 75 μm column terminating in an 8.5 μm tip, was run at $\sim$200 nl/min. During chromatography, the ion trap repetitively surveyed full-scan MS over the range of 395–1400 m/z, executing data-dependent scans on the three most abundant ions in the survey scan. MS/MS spectra were acquired with a relative collision energy of 30%, an isolation width of 2.5 Dalton, and recurring ions dynamically excluded. Interpretation of peptide MS/MS spectra was facilitated by database correlation us-ing SEQUEST and programs developed in the Harvard Microchemis-try Facility (Chittum et al., 1998; Eng et al., 1994).

Molecular Cloning of ICIS

Nucleotides 2059–3369 of the ICIS coding region were PCR ampli-fied from a *Xenopus* ovary cDNA library (a gift from A. Straight, Harvard Medical School), and used to screen the same library. Four overlapping clones were partially sequenced, and the one con-taining the largest insert (clone 10) was fully sequenced and used for the remainder of our studies.

Purification of Recombinant Proteins from *E. coli* and Antibody Preparation

His$_6$-ICIS.C1, composed of ICIS amino acids 727–1065 fused to an N-terminal His$_6$ tag, was expressed in *E. coli* BL21DE3 cells, purified with Ni^{2+}-NTA agarose (Qiagen), and used to immunize rabbits (Co-calico Biologicals). ICIS-specific antibodies were affinity purified over Affi-Gel 10 (Bio-Rad) covalently linked to His$_6$-ICIS.C1. Antibod-ies used to block ICIS function in *Xenopus* extracts were dialyzed into 10 mM K-HEPES (pH 7.7), 100 mM KCl, concentrated to 11.4 mg/ml using Centricons (Millipore), and frozen in liquid nitrogen following addition of sucrose to 150 mM. Alexa 594- or 488-α-ICIS conjugates were prepared as suggested by the manufacturer (Mo-lecular Probes).

Xenopus Skp1, PCR-amplified from the library described above, and MCAK^{NT} (residues 2–264; a gift from C. Walczak, Indiana Univer-sity, Bloomington) were expressed in BL21DE3 cells as GST-fusions and purified on glutathione agarose (Sigma). GST was similarly ex-pressed and purified. Aggregates of GST and GST-MCAK^{NT} were removed by gel filtration on a Superose 12 column (Amersham Bio-sciences) equilibrated in 10 mM K-HEPES (pH 7.7), 200 mM KCl, 1 mM DTT before use in spindle assembly experiments. GST-Skp1 was used to immunize rabbits (Cocalico Biologicals). α-Skp1 anti-bodies were affinity purified by passing α-GST-depleted serum over Affi-Gel 10 covalently coupled to GST-Skp1.

Polyclonal rabbit α-*Xenopus* Aurora B-CTP antibodies were raised to the C-terminal 20 amino acids of XAurora B (WVKANSRRVLPP VYQSTQSK; Research Genetics), and affinity purified against the same peptide.

Spindle Assembly in *Xenopus* Extracts

Metaphase bipolar spindles were assembled in CSF and cycled extracts as described (Desai et al., 1999a) in the presence of 50 μg/ml X-rhodamine-labeled tubulin (Hyman et al., 1991) to visualize microtubules. Demembranated *Xenopus* sperm nuclei (Murray, 1991) were used at 200/μl of extract for antibody addition experi-ments and 400/μl of extract for all other experiments.

To block ICIS function during spindle assembly, α-ICIS or nonspe-cific rabbit IgG (Jackson Immunoresearch Laboratories) at 11.4 mg/ml were added to CSF extracts to 0.75 mg/ml. Sperm nuclei and 0.4 mM CaCl$_2$ were added to induce mitotic exit and chromosome replication. Eighty minutes later, 0.75 volumes of CSF extract con-taining the appropriate antibodies were added to the cycled ex-tracts. Assembled structures were analyzed 90 min later by squash-ing 1 μl of extract mixed with 4 μl of fix (Murray, 1991) underneath an 18 $\times$ 18 mm coverslip and viewing the sample by fluorescence microscopy. To perturb ICIS function in preassembled spindles, IgG or α-ICIS were added to extract containing metaphase spindles to 0.5 mg/ml.

Inhibition of MCAK inner centromere targeting was accomplished by supplementing CSF extract with GST-MCAK^{NT} or, as a control, GST to 250 μg/ml prior to initiating spindle assembly reactions. Replicated metaphase chromosomes were prepared by cycling

sperm nuclei through extract as described above with 50 μM noco-dazole to prevent microtubule assembly.

Immunofluorescence Microscopy

Xenopus XTC cells cultured on poly-L-lysine-coated coverslips were simultaneously permeabilized and fixed in 100 mM K-PIPES (pH 6.8), 10 mM EGTA, 1 mM MgCl$_2$, 0.2% Triton X-100, 3% formaldehyde for 10 min. Spindles and mitotic chromatin assembled in *Xenopus* extracts were processed for immunofluorescence as described (De-sai et al., 1999a). Coverslips were blocked in AbDil (Tris-buffered saline plus 0.1% Triton X-100, 2% BSA) for 30 min. Primary antibod-ies diluted in AbDil were incubated with coverslips for 1 hr. When necessary, fluorophore-conjugated secondary antibodies (Molecu-lar Probes) were diluted 1:500 in AbDil and incubated with coverslips for 45 min. For costaining of ICIS and Aurora B, the following anti-bodies were incubated with coverslips: α-XAurora B-CTP, Alexa 594-α-rabbit, 1 mg/ml rabbit IgG, and Alexa 488-α-ICIS. The follow-ing were used at 1 μg/ml: Alexa 488- and Alexa 594-α-ICIS, Alexa 594-α-XCENP-E (a gift from A. Straight), α-XAurora B-CTP, Oregon green-α-XMCAK, and α-XMCAK-CTP (a gift from C. Walczak). Monoclonal α-tubulin FITC-conjugated DM1α antibody (Sigma) was used at 1:500. After staining DNA with 5 μg/ml Hoechst 33342, coverslips were mounted in 90% glycerol, 0.5% p-phenylenedia-mine, 20 mM Tris-Cl (pH 8.8) and imaged by wide-field fluorescence microscopy using a Nikon E800 microscope equipped with a 100$\times$ 1.4 NA objective or an Olympus IX70 inverted microscope using a 60$\times$ 1.4 NA objective. Inverted microscope images were taken at 0.2 μm z-steps, and used to produce deconvolved reconstructions of the image stacks (Agard et al., 1989), which are presented as maximum intensity projections.

Electron Microscopy

To best preserve kinetochore and kinetochore fiber structure, spin-dles were fixed with 25 mM lysine, 1.5% glutaraldehyde. For immu-noelectron microscopy, spindles were assembled in the presence of 10 μg/ml α-ICIS, which labels ICIS at inner centromeres without disrupting spindle assembly. ICIS-labeled spindles were fixed with 2% formaldehyde, 0.25% glutaraldehyde in 30% glycerol/BRB80 for 10 min, and sedimented onto poly-L-lysine-coated, glow-dis-charged Aclar coverslips (Ted Pella). Samples were blocked with 0.1% gelatin in AbDil for 1 hr and incubated with goat α-rabbit IgG Fab fragment conjugated to nanogold (Molecular Probes) at 1 μg/ml in AbDil overnight at 4°C. Following washes with BRB80 and water, samples were silver enhanced for 5 min with IntenSE (Amer-sham Biosciences).

Coverslips were then incubated in the following solutions pre-pared in 50 mM cacodylate buffer (pH 7.0): 25 mM lysine, 1.5% glutaraldehyde, 6 min; 1.5% glutaraldehyde, 12 min; and 1% os-mium, 0.8% K-ferricyanide, 15 min, at 0°C. Samples were stained in 1% uranyl acetate for 2 hr at 4°C and dehydrated by temperature reduction in an ethanol series. At 100% ethanol, coverslips were brought to room temperature and infiltrated using 2:1, 1:2 propylene oxide:epon araldite, followed by 100% epon araldite, and then mounted and polymerized at 65°C for 48 hr. Spindles, selected mi-croscopically, were remounted for sectioning at 85 nm intervals using a DMK diamond knife (kindly provided by Drukker) on a Reichert Ultracut S microtome. Spindles were viewed and imaged on a JOEL 1200 electron microscope.

Purification of Recombinant ICIS and *Xenopus* MCAK

A ZZ-TEV$_4$ tag (Stemmann et al., 2001) was appended to the N terminus of ICIS by subcloning the ICIS coding sequence into pOS135 (a gift from O. Stemmann, Max Planck Institute of Biochem-istry). The sequence encoding ZZ-TEV$_4$-ICIS was transferred into pFASTBAC1 (Invitrogen) and the resulting clone was used to pro-duce a baculovirus as detailed by the Bac-to-Bac system (In-vitrogen). To purify ICIS, infected *Sf*-9 cells expressing ZZ-TEV$_4$-ICIS were lysed in 20 mM Tris-Cl (pH 7.7), 500 mM NaCl, 1% IGEPAL CA-630, 1 mM EDTA, LPC, 1 mM PMSF, 1 mM benzamidine and clarified by centrifugation at 147,505 $\times$ g for 1 hr. One milliliter of IgG Sepharose (Amersham Biosciences) was rotated with the supernatant for 1 hr at 4°C, washed with 20 mM Tris-Cl (pH 7.7), 500 mM NaCl, 0.5% IGEPAL CA-630, 1 mM EDTA, followed by 10 ml of cleavage buffer (10 mM Tris-Cl [pH 8], 300 mM NaCl, 0.1% IGEPAL CA-630, 0.5 mM EDTA, 1 mM DTT). ICIS was eluted by

resuspending the resin in 2 ml cleavage buffer plus 150 μg of GST-TEV protease and incubating the slurry at 22°C for 1 hr. GST-TEV protease was removed with glutathione agarose and ICIS was desalted into 10 mM K-HEPES (pH 7.7), 300 mM KCl, 1 mM DTT, 1 mM MgCl$_2$, 1 mM EGTA and concentrated. Sucrose was added to 20%, and the protein was aliquoted, frozen in liquid nitrogen, and stored at −80°C.

Untagged *Xenopus* MCAK was expressed in *Sf*-9 cells using a previously reported baculovirus (Desai et al., 1999b) and purified by ion exchange and gel filtration chromatography as described (Desai et al., 1999b).

Visual Analysis of GMPCPP-Microtubule Depolymerization

Xenopus MCAK (225 nM) was incubated with ICIS (750 nM) at 0°C for 10 min in 25 mM K-HEPES (pH 7.7), 150 mM KCl, 1 mM DTT, 1 mM MgCl$_2$, 1 mM EGTA, 100 μg/ml casein and then added to a reaction mixture containing ∼440 nM rhodamine-labeled GMPCPP-microtubules (1.5 μM tubulin; 1:5 labeled:unlabeled tubulin) in BRB80 plus 75 mM KCl, 1 mM MgATP, 1 mM DTT, 100 μg/ml casein. The concentrations of MCAK and ICIS in these reactions were 15 nM and 50 nM, respectively. Titration of ICIS activity was accomplished by serial dilution of ICIS, addition of 225 nM MCAK, incubating the proteins at 0°C for 10 min, and then assembling the reactions as described above. Reactions were monitored by squashing 1 μl of each sample underneath 18 × 18 mm coverslips and observing them by fluorescence microscopy through a Nikon 60× 1.4 NA objective. Images were recorded with a cooled CCD and Metamorph software (Universal Imaging Corporation) using identical exposure parameters.

ICIS-Microtubule Cosedimentation Assay

Preclarified 25 nM ICIS was mixed with taxol-stabilized GTP-microtubules or unpolymerized tubulin (1 μM) in BRB80 plus 100 mM KCl, 1 mM DTT, 1 μM taxol and incubated at 22°C for 15 min. Binding reactions were centrifuged over 40% sucrose/BRB80 plus 100 mM KCl, 1 μM taxol at 118,241 × g for 20 min at 20°C. ICIS and tubulin in the pellet and supernatant fractions were analyzed by immunoblotting.

Immunoprecipitations and Immunoblotting

For immunoprecipitations, α-ICIS or rabbit IgG was crosslinked to Affi-Prep protein A (Bio-Rad) with dimethyl pimelimidate (Pierce) as described (Harlow and Lane, 1988) using 1.6 μg of antibody/μl of beads. Beads (7.5 μl) were washed three times with CSF-XB and incubated in 250 μl of CSF extract for 1 hr at 4°C. Beads were washed twice with CSF-XB, six times with NP-40 buffer (10 mM Na phosphate [pH 7.2], 150 mM NaCl, 2 mM EDTA, 1% IGEPAL CA-630), boiled in sample buffer, and analyzed by SDS-PAGE.

Immunoblots, blocked with 5% w/v skim milk in TBS, were probed with primary antibodies diluted to 1 μg/ml (α-ICIS, α-XMCAK, α-INCENP [a gift from A. Straight], and α-Skp1); 1:2000 for α-Aurora B (a gift from T. Stukenberg); or 1:1000 for α-tubulin DM1α. Antibodies were detected by enhanced chemiluminescence (Amersham Biosciences).

References

Adams, R.R., Carmena, M., and Earnshaw, W.C. (2001). Chromosomal passengers and the (aurora) ABCs of mitosis. Trends Cell Biol. *11*, 49–54.

Agard, D.A., Hiraoka, Y., Shaw, P., and Sedat, J.W. (1989). Fluorescence microscopy in three dimensions. Methods Cell Biol. *30*, 353–377.

Bai, C., Sen, P., Hofmann, K., Ma, L., Goebl, M., Harper, J.W., and Elledge, S.J. (1996). SKP1 connects cell cycle regulators to the ubiquitin proteolysis machinery through a novel motif, the F-box. Cell *86*, 263–274.

Buvelot, S., Tatsutani, S.Y., Vermaak, D., and Biggins, S. (2003). The budding yeast Ipl1/Aurora protein kinase regulates mitotic spindle disassembly. J. Cell Biol. *160*, 329–339.

Cassimeris, L. (1999). Accessory protein regulation of microtubule dynamics throughout the cell cycle. Curr. Opin. Cell Biol. *11*, 134–141.

Chittum, H.S., Lane, W.S., Carlson, B.A., Roller, P.P., Lung, F.D., Lee, B.J., and Hatfield, D.L. (1998). Rabbit β-globin is extended beyond its UGA stop codon by multiple suppressions and translational reading gaps. Biochemistry *37*, 10866–10870.

Cimini, D., Howell, B., Maddox, P., Khodjakov, A., Degrassi, F., and Salmon, E.D. (2001). Merotelic kinetochore orientation is a major mechanism of aneuploidy in mitotic mammalian tissue cells. J. Cell Biol. *153*, 517–527.

Cleveland, D.W., Mao, Y., and Sullivan, K.F. (2003). Centromeres and kinetochores: from epigenetics to mitotic checkpoint signaling. Cell *112*, 407–421.

Cooke, C.A., Heck, M.M., and Earnshaw, W.C. (1987). The inner centromere protein (INCENP) antigens: movement from inner centromere to midbody during mitosis. J. Cell Biol. *105*, 2053–2067.

Desai, A., and Mitchison, T.J. (1997). Microtubule polymerization dynamics. Annu. Rev. Cell Dev. Biol. *13*, 83–117.

Desai, A., Murray, A., Mitchison, T.J., and Walczak, C.E. (1999a). The use of *Xenopus* egg extracts to study mitotic spindle assembly and function in vitro. Methods Cell Biol. *61*, 385–412.

Desai, A., Verma, S., Mitchison, T.J., and Walczak, C.E. (1999b). Kin I kinesins are microtubule-destabilizing enzymes. Cell *96*, 69–78.

Eng, J.K., McCormack, A.L., and Yates, J.R., III. (1994). An approach to correlate tandem mass spectral data of peptides with amino acid sequences in a protein database. J. Am. Soc. Mass Spectrom. *5*, 976–989.

Gard, D.L., and Kirschner, M.W. (1987). A microtubule-associated protein from *Xenopus* eggs that specifically promotes assembly at the plus-end. J. Cell Biol. *105*, 2203–2215.

Harlow, E., and Lane, D. (1988). Antibodies: A Laboratory Manual (Cold Spring Harbor, NY: Cold Spring Harbor Laboratory Press).

Holy, T.E., and Leibler, S. (1994). Dynamic instability of microtubules as an efficient way to search in space. Proc. Natl. Acad. Sci. USA *91*, 5682–5685.

Hunter, A.W., Caplow, M., Coy, D.L., Hancock, W.O., Diez, S., Wordeman, L., and Howard, J. (2003). The kinesin-related protein MCAK is a microtubule depolymerase that forms an ATP-hydrolyzing complex at microtubule ends. Mol. Cell *11*, 445–457.

Hyman, A.A., and Karsenti, E. (1996). Morphogenetic properties of microtubules and mitotic spindle assembly. Cell *84*, 401–410.

Hyman, A., Drechsel, D., Kellogg, D., Salser, S., Sawin, K., Steffen, P., Wordeman, L., and Mitchison, T. (1991). Preparation of modified tubulins. Methods Enzymol. *196*, 478–485.

Jensen, C.G. (1982). Dynamics of spindle microtubule organization: kinetochore fiber microtubules of plant endosperm. J. Cell Biol. *92*, 540–558.

Kallio, M.J., McCleland, M.L., Stukenberg, P.T., and Gorbsky, G.J. (2002). Inhibition of aurora B kinase blocks chromosome segregation, overrides the spindle checkpoint, and perturbs microtubule dynamics in mitosis. Curr. Biol. *12*, 900–905.

Karsenti, E., and Vernos, I. (2001). The mitotic spindle: a self-made machine. Science *294*, 543–547.

Kinoshita, K., Arnal, I., Desai, A., Drechsel, D.N., and Hyman, A.A. (2001). Reconstitution of physiological microtubule dynamics using purified components. Science *294*, 1340–1343.

Kirschner, M., and Mitchison, T. (1986). Beyond self-assembly: from microtubules to morphogenesis. Cell *45*, 329–342.

Kline-Smith, S.L., and Walczak, C.E. (2002). The microtubule-destabilizing kinesin XKCM1 regulates microtubule dynamic instability in cells. Mol. Biol. Cell *13*, 2718–2731.

Maney, T., Hunter, A.W., Wagenbach, M., and Wordeman, L. (1998). Mitotic centromere-associated kinesin is important for anaphase chromosome segregation. J. Cell Biol. *142*, 787–801.

McDonald, K.L., O'Toole, E.T., Mastronarde, D.N., and McIntosh, J.R. (1992). Kinetochore microtubules in PTK cells. J. Cell Biol. *118*, 369–383.

Murray, A.W. (1991). Cell cycle extracts. Methods Cell Biol. *36*, 581–605.

Nasmyth, K., Peters, J.M., and Uhlmann, F. (2000). Splitting the chromosome: cutting the ties that bind sister chromatids. Science *288*, 1379–1385.

Nicklas, R.B. (1997). How cells get the right chromosomes. Science *275*, 632–637.

Regan-Reimann, J.D., Duong, Q.V., and Jackson, P.K. (1999). Identification of novel F-box proteins in *Xenopus laevis*. Curr. Biol. *9*, R762–R763.

Rieder, C.L., and Salmon, E.D. (1994). Motile kinetochores and polar ejection forces dictate chromosome position on the vertebrate mitotic spindle. J. Cell Biol. *124*, 223–233.

Rieder, C.L., and Salmon, E.D. (1998). The vertebrate cell kinetochore and its roles during mitosis. Trends Cell Biol. *8*, 310–318.

Scholey, J.M., Brust-Mascher, I., and Mogilner, A. (2003). Cell division. Nature *422*, 746–752.

Shannon, K.B., and Salmon, E.D. (2002). Chromosome dynamics: new light on aurora B kinase function. Curr. Biol. *12*, R458–R460.

Stemmann, O., Zou, H., Gerber, S.A., Gygi, S.P., and Kirschner, M.W. (2001). Dual inhibition of sister chromatid separation at metaphase. Cell *107*, 715–726.

Tanaka, T.U. (2002). Bi-orienting chromosomes on the mitotic spindle. Curr. Opin. Cell Biol. *14*, 365–371.

Walczak, C.E., Mitchison, T.J., and Desai, A. (1996). XKCM1: a *Xenopus* kinesin-related protein that regulates microtubule dynamics during mitotic spindle assembly. Cell *84*, 37–47.

Walczak, C.E., Gan, E.C., Desai, A., Mitchison, T.J., and Kline-Smith, S.L. (2002). The microtubule-destabilizing kinesin XKCM1 is required for chromosome positioning during spindle assembly. Curr. Biol. *12*, 1885–1889.

Wood, K.W., Sakowicz, R., Goldstein, L.S., and Cleveland, D.W. (1997). CENP-E is a plus end-directed kinetochore motor required for metaphase chromosome alignment. Cell *91*, 357–366.

Wordeman, L., and Mitchison, T.J. (1995). Identification and partial characterization of mitotic centromere-associated kinesin, a kinesin-related protein that associates with centromeres during mitosis. J. Cell Biol. *128*, 95–104.

Accession Numbers

The GenBank accession number for the nucleotide sequence of *Xenopus* ICIS reported in this paper is AY352638.